International Journal of Thermal Sciences 49 (2010) 196–201

Contents lists available at ScienceDirect

International Journal of Thermal Sciences

journal homepage: www.elsevier.com/locate/ijts

Thermal analysis and optimization of multiple LED packaging based on a general analytical solution

Ting Cheng [a], Xiaobing Luo [a,b,*], Suyi Huang [a], Sheng Liu [b]

[a] School of Energy and Power Engineering, Huazhong University of Science & Technology, Wuhan 430074, China
[b] Wuhan National Lab for Optoelectronics, Huazhong University of Science & Technology, Wuhan 430074, China

ARTICLE INFO

Article history:
Received 28 October 2008
Received in revised form
12 July 2009
Accepted 13 July 2009
Available online 31 July 2009

Keywords:
LEDs
Thermal spreading resistance
Analytical solution

ABSTRACT

Multiple-chip packaging becomes common in LEDs packaging community. For such type of packaging, thermal spreading resistance is an important factor to affect the total thermal performance of LEDs. In this study, a general analytical solution is used to study the whole temperature field of LED packaging substrate, this solution is based on the method of variable separation for thermal spreading resistances of eccentric heat sources on a rectangular flux channel. The feasibility of the analytical method used in LEDs packaging has been proven by the temperature comparison with existing experimental and numerical results of an 80 W LED street lamp. By changing the chips arrangement on the substrate, temperature field optimization is conducted with maximal temperature difference of the substrate as the target function. The results show that spreading resistance plays a significant role to affect temperature field. When the LED distributions are effectively designed, the highest temperature on the substrate goes lower and the lowest temperature on the board goes higher, the temperature field becomes uniform, its spreading resistance becomes lower.

© 2009 Elsevier Masson SAS. All rights reserved.

1. Introduction

Lighting-emitting diodes (LEDs) have many significant advantages, such as high efficiency, good reliability, long lifetime, variable color and low power consumption, therefore, LEDs have begun to play an important role in many applications [1]. Typical applications include back lighting for cell phones and other liquid crystal display (LCD), interior and exterior automotive lighting illumination. In the near future, the biggest area that LED will be used in is general lighting. In energy shortage condition, Chinese authorities estimate that if LEDs dominate the lighting market in 2010, one third of the present lighting power consumption will be saved, which will greatly ameliorate the energy crisis in China [2].

To obtain more lumen, the driving electric current of LED chips grows fastly nowadays. However, as to the high power LED chips, generally nearly 80% of the input power is transformed into heat while the rest is transformed into light. Therefore, during the effort to make LED brighter, lots of heat in LED chips will be generated. Inevitably, the temperature of the LED chips will increase because of this heat. Temperature of LEDs is a primary parameter influencing the reliability and durability [3], high temperature and temperature gradient will generate significant stresses in both materials and along interfaces, if considering the mismatch of Young's modules and coefficients of thermal expansions (CTEs). Exceeding the maximum rated chip temperature could lead to accelerated light output degradation and sometimes even catastrophic failure. Moreover, LED temperature influences the light output quality. Therefore, to gain a reliable and perfect product with good performance, thermal management of high power LEDs is very important. Temperature of LED chip is a key evaluation parameter of thermal management.

In order to meet the illuminating demand and reduce the cost, LEDs have been packaged in multi-chip packaging modules. Thermal performances of multi-chip modules are different from single chip modules due to the possible non-uniformity in temperature. Research on thermal characteristic of multi-chip LEDs is becoming a new topic. Kim and Shin have introduced the thermal difference of one-chip, two-chip and four-chip designs [4]. The results demonstrate that in multi-chip packaging, the dependence of the thermal resistance and junction temperature on the number of the chips is stronger for the LED package.

For the multi-chip packaging design, spreading thermal resistance should be considered [5,6]. Thermal spreading resistance theory is found to have widespread applications in electronics cooling, both at the board and chip level. These include, but are not

* Corresponding author. School of Energy and Power Engineering, Huazhong University of Science & Technology, Wuhan 430074, China. Tel.: +86 13971460283; fax: +86 27 87557074.
E-mail address: luoxb@mail.hust.edu.cn (X. Luo).

1290-0729/$ – see front matter © 2009 Elsevier Masson SAS. All rights reserved.
doi:10.1016/j.ijthermalsci.2009.07.010

Nomenclature

a,b,c,d	linear dimensions, m
A_b	baseplate area, m^2
A_s	heat source area, m^2
A_0,A_m,A_n,A_{mn}	Fourier coefficients
B_i	Biot number, hl/k
C_p	specific heat capacity,J/kg K
I	index denoting layers 1 and 2
H	heat transfer coefficient, W/m^{2}K
h_{eff}	equivalent natural convection efficient
k	thermal conductivity, W/mK
m,n	indices for summations
Q	heat flow rate, W
q	heat flux, W/m^2
$\beta_{m,n}$	eigenvalue, $\equiv\sqrt{\lambda_m^2+\delta_n^2}$
δ_n	eigenvalue, $(n\pi/b)$
T	temperature on plate, K
T_f	sink temperature, K
θ	temperature excess, $\equiv T-T_f$, K

limited to, the prediction of thermal resistance of electronic devices known as ball grid arrays [7], the effect of heat source eccentricity [8], the effect of heat spreaders in compound systems [9–12], the effect of orthotropic properties [13,14], and the issues of contact shape and edge cooling [15–17]. In a multi-chip packaging, huge heat generated from the LED chips is conducted through heat slug to the printed circuit board, and finally is transferred from the heat sink to environment. Thermal spreading resistance of multi-chip packaging which results from discrete heat sources is a key thermal resistance in the above heat transfer process. Yovanovich and Culham's group has many researches on the spreading resistance of multi-chip packaging, specially in the applications of electronic packaging and reliability. In these studies, Muzychka et al. [8] have proposed a simple method for predicting mean and centroidal heat source temperature. The influence of spreading thermal resistance in multi-chip packaging has also been studied theoretically by means of an influence coefficient [18].

With different needs and conditions, there are several direct and indirect methods to study LED chip temperature. Numerical simulation [2,19] and experimental test including forward-voltage method [20], micro-Raman spectroscopy [21], electro luminescence [22] and thermocouple measurement [2], are used to understand the heat transfer performance of LEDs. They are based on different theories and focused on different aspects. However, every method mentioned above has some limitations. Experiment is just suitable for the forthcoming sample and always depends on the apparatus. It is also difficult to show the whole-field temperature based on the experimental data. Numerical simulation method needs professional knowledge of modeling and simulations and, to a large degree, its result accuracy is determined by the prescription of simulation boundary conditions.

Considering the deficiency of aforementioned methods and the thermal spreading resistance of multi-chip packaging, a general analytical solution calculating the thermal spreading resistance is used to analyze thermal characteristic of multi-chip LED packaging in this study. Heat transfer optimization has also been carried out to achieve a uniform temperature field based on this method.

2. Description of analytical solution

Muzychka et al. have presented an analytical general solution based on separation variable method for total thermal spreading resistance of eccentric heat sources on rectangular flux channel [8]. The solution is

$$\theta(x,y,z) = T(x,y,z) - T_f \tag{1}$$

where $T(x,y,z)$ is the layer temperature, and T_f is the sink temperature. This solution can be used to model any number of discrete heat sources on a compound or an isotropic flux channel. It is finally expressed as

$$\begin{aligned}\theta(x,y,z) = {} & A_0 + B_0 z + \sum_{m=1}^{\infty}\cos(\lambda x)[A_1\cosh(\lambda z) + B_1\sinh(\lambda z)] \\ & + \sum_{n=1}^{\infty}\cos(\delta y)[A_2\cosh(\delta z)B_2\sinh(\delta z)] + \sum_{m=1}^{\infty} \\ & \times \sum_{n=1}^{\infty}\cos(\lambda x)\cos(\delta y)[A_3\cosh(\beta z) + B_3\sinh(\beta z)]\end{aligned} \tag{2}$$

where $\lambda = m\pi/a$, $\delta = n\pi/b$, and $\beta = \sqrt{\lambda^2+\delta^2}$.

From the above equation, it is found that it contains four components, a uniform flow solution and three spreading solutions which vanish when the heat flux is distributed uniformly over the entire surface $z = 0$. Application of the thermal boundary condition at $z = t_1$ for an isotropic rectangular plate yields the following result for the Fourier coefficients

$$B_i = -\phi(\zeta)A_i \quad i = 1,2,3 \tag{3}$$

where

$$\phi(\zeta) = \frac{\zeta\sinh(\zeta t_1) + h/k_1\cosh(\zeta t_1)}{\zeta\cosh(\zeta t_1) + h/k_1\sinh(\zeta t_1)} \tag{4}$$

where ζ is replaced by λ,δ,β. The final coefficientsA_m,A_n,A_{mn} are obtained by taking Fourier series expansions of boundary condition at the surface $z = 0$. This results in the following equations

$$A_m = \frac{2Q\left[\sin\left(\frac{2X_c+c}{2}\lambda_m\right) - \sin\left(\frac{2X_c-c}{2}\lambda_m\right)\right]}{abck_1\lambda_m\phi(\lambda_m)} \tag{5}$$

$$A_n = \frac{2Q\left[\sin\left(\frac{2Y_c+d}{2}\right)\delta_n - \sin\left(\frac{2Y_c-d}{2}\right)\delta_n\right]}{abdk_1\delta_n\phi(\delta_n)} \tag{6}$$

$$A_{mn} = \frac{16Q\cos(\lambda_m X_c)\sin(\frac{1}{2}\lambda_m c)\cos(\delta_n Y_c)\sin(\frac{1}{2}\delta_n d)}{abcdk_1\beta_{m,n}\lambda_m\delta_n\phi(\beta_{m,n})} \tag{7}$$

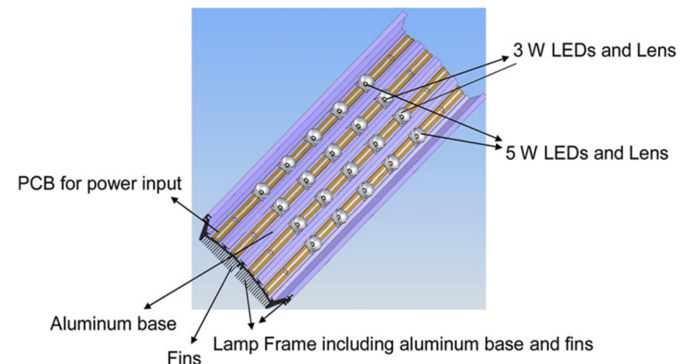

Fig. 1. Schematic diagram of the 80 W LED street lamp.

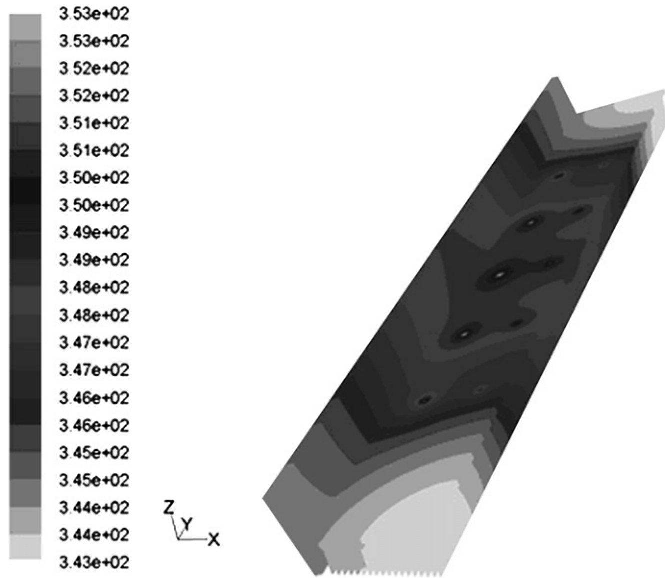

Fig. 2. Temperature distribution at the environment temperature of 45 °C.

Finally, values for the coefficients in the uniform flow solution are given by

$$A_0 = \frac{Q}{ab}\left(\frac{t_1}{k_1}+\frac{1}{h}\right) \tag{8}$$

$$B_0 = -\frac{Q}{k_1 ab} \tag{9}$$

For multiple heat sources, the solution for the temperature distribution on the surface of the board or heat sink is obtained using superposition. Therefore, there is

$$\theta_i(x,y,0) = A_0^i + \sum_{m=1}^{\infty} A_m^i \cos(\lambda x) + \sum_{m=1}^{\infty} A_n^i \cos(\delta y) + \sum_{m=1}^{\infty} \times \sum_{n=1}^{\infty} A_{mn}^i \cos(\lambda x)\cos(\delta y) \tag{10}$$

where θ_i is the temperature excess for each heat sources by itself. By adding each θ_i, it is easy to obtain the temperature of each heat sources and the temperature distribution on board or heat sink.

3. Temperature calculation of an 80W LED street lamp

Experiment and numerical simulation of an 80W LED street lamp shown in Fig. 1 have been conducted in the authors' previous work [2]. The lamp is mainly composed of three parts: twenty high-power LED modules, a mechanical frame for heat dissipation and supporting LED modules. The lamp frame consists of an aluminum base and aluminum fins. Twenty high-power LED modules are directly bonded to the aluminum base. The modules in the central two rows are 3 W LED packaging, each of which includes three 1 W chips inside. The other two rows consist of 5 W LED modules, each of the 5 W packages includes four chips inside, and they are supplied with 5 W power. In the former experiment study, sixteen thermocouples were used to measure the temperature points at the aluminum base and fins. Based on experimental data, the average heat transfer coefficient of natural convection on the lamp is obtained. A numerical model was also proposed based on the experiment results to show the whole temperature field of the lamp. According to the temperature field of numerical analysis shown in Fig. 2, the temperature changes a wide scale in the whole model. It is obvious that a large temperature difference exists between the chip location and the substrate edge. Therefore, spreading resistance cannot be ignored in this multi-chip packaging lamp.

The heat transfer characteristics inside the street lamp are as follows: firstly, LED chip is the heat source; secondly, LED chips are

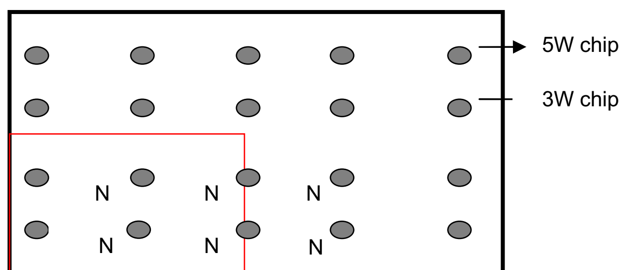

Fig. 3. Schematic of the calculation chips distribution.

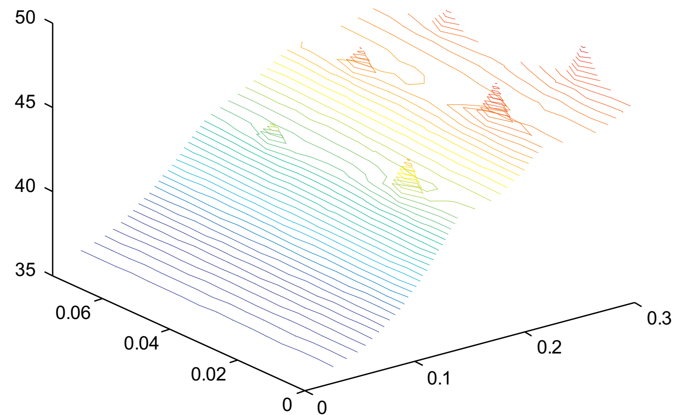

Fig. 4. 3D temperature field of quarter part of street lamp heat sink plate.

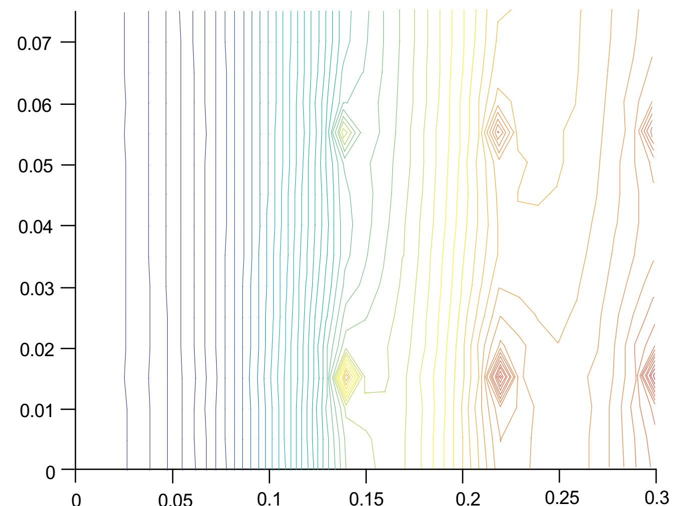

Fig. 5. 2D temperature field of quarter part of street lamp heat sink plate. ($Z = 0$ cross section).

Table 1
Temperature data of six peaks (°C).

	Under 3 W chip		Under 5 W chip	
Row 1 chip	No.1	41.6	No. 2	42.1
Row 2 chip	No. 3	44.7	No. 4	45.4
Row 3 chip	No. 5	45.6	No. 6	46.1

eccentric heat sources on rectangular channel; thirdly, LED packaging is based on electronic packaging method and its thermal management methods are mainly heat conduction and convection. According to the heat transfer analysis and the description of the analytical general solution, the equation in the above section is supposed to be suitable to calculate the thermal spreading resistance of this lamp.

In the solution presented by Muzychka et al., eccentric heat sources are on rectangular flux channel, the whole model is a rectangular plate, but in the lamp shown in Fig. 1, the mechanical frame of the lamp is a complicated structure, which needs model simplification. Its heat sink needs to be simplified into a flat plate. Twenty one LED chips in this model are simplified into twenty-one squares, whose sizes are 1 mm by 1 mm. The convection coefficient of the bottom surface on the simplified plate is replaced by an equivalent value which accounts for both the heat transfer in the fin surface and the plate surface. The other faces encapsulated in lampshade, are supposed to be adiabatic, because there is little part of heat flux passing through them.

To apply the above equations into the present model, heat sink with many fins should be simplified into a plate in heat transfer area. c and d is the length and width of the heat source respectively, which is 1 mm here. α is the real heat transfer coefficient based on the heat sink area including fin area. According to the experimental data obtained in the previous work [2] and based on $Q = \alpha F \nabla T$, the average heat transfer coefficient of natural convection on the lamp is obtained as follows

$$\alpha = \frac{Q}{F \nabla T} = \frac{70}{1.2*(42-11)} \mathrm{W/m^2} \quad K = 1.9\,\mathrm{W/m^2K}$$

where Q is the heat, F is the total heat transfer area of the lamp fins and base, which is about 1.2 m^2. ∇T is the temperature difference between the fin and the environment. In the experiments, the steady average temperature of the fin and base was about 42.1 °C. The environment temperature was about 11 °C. Thus, ∇T is about 31 K. Then its general convection coefficient is 1.9 W/(m^{2}K). In this case, heat sink is simplified into a flat plate (0.6 m by 0.3 m) with the bottom face area of 2.032 m^2. h_{eff} is an equivalent natural convection efficient when the heat sink of the street lamp is regarded as a plate without its fins. The relationship between α and h_{eff} is described as $A\alpha = h_{\mathrm{eff}} A_b$. A is the total heat sink area that is exposed to the environment. A_b is the heat sink base area, and it does not include the fin area. Based on the equation, equivalent convection coefficient h_{eff} in this simplified model is 25.344 W/(m^{2}K), which depends on fin base area.

After obtaining the basic parameters, a MATLAB program is built to calculate the above equations (1)–(10) and draw the isothermal chart. Firstly, it calculates the temperature excess θ_i, which is caused by the ith LED chip, then adds all θ_i and ambient temperature to obtain the temperature of the whole LED street lamp. The material of the lamp structure is aluminum, and its thermal conductivity is 160 W/mK.

Table 2
Temperature comparison under two chip distribution cases.

	Highest temperature (°C)	Lowest temperature (°C)	Temperature difference (°C)
One chip distribution case	48.4	36.3	12.1
Another chip distribution case	45.6	40.1	5.5

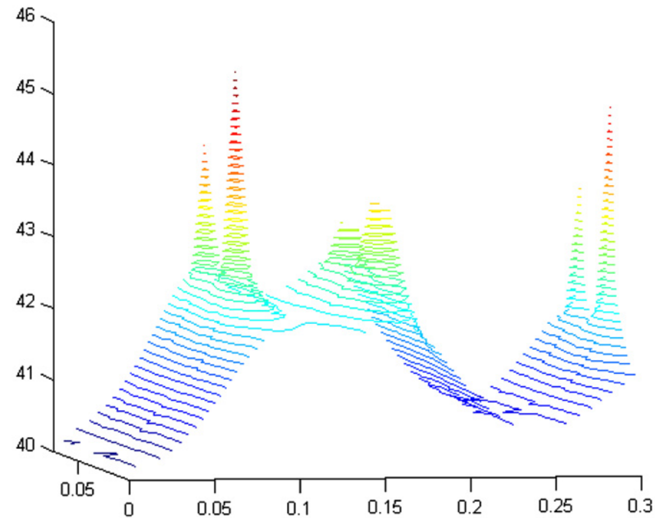

Fig. 6. 3D temperature field of quarter part of street lamp heat sink plate with 5.54 °C maximal temperature difference.

As the plate is axis symmetric structure, to save calculation time, temperature field of a quarter of the simplified plate area is shown. The calculation section is shown in Fig. 3. Isothermal chart made by the MATLAB program is shown in Figs. 4 and 5.

It is clear from Figs. 4 and 5 that there are six peaks in the temperature field. They are the hottest areas where the LED chips are located. The temperature data of the six peaks is presented in Table 1.

With the same ambient temperature, experimental temperature tested by thermocouple located near the 5 W chip in row 1 is 42.1 °C, and in numerical analysis the corresponding temperatures are 47.11 °C (5 W chip) and 46.11 °C (3 W chip). There are differences between these hottest temperatures obtained by three methods. Temperature calculated by the analytical general solution is much closer to the data obtained by numerical analysis. These differences can be attributed to the measurement location difference. Experiment data was collected by thermocouples placed around LED chip modules. Thermocouples were located next to the chip module and kept small distance from heat generation points, which is due to the limitation of thermocouple distribution.

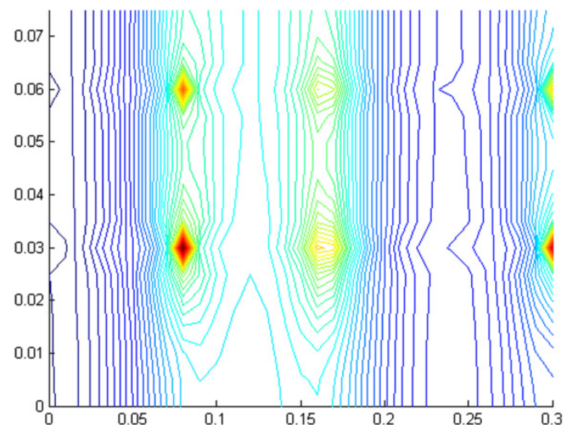

Fig. 7. 2D temperature field of quarter part of street lamp heat sink plate with 5.54 °C maximal temperature difference.

Table 3
X coordinate of the chip locations (m).

Old	0.14	0.22	0.3	0.38	0.46
New	0.06	0.18	0.3	0.42	0.54

Therefore, the temperature measured by thermocouples was of the surface on heat sink plate which was near the chip, rather than exact chip location temperature. However, for simulation and analytical results, both the temperature data are of the location where actual LED chip was bonded.

To sum up, a general analytical solution can be used to analyze thermal characteristics of the LEDs in multi-chip packaging. It can provide relatively accurate data. Comparing with the above two methods, the present analysis needs less resource and time, it just need do a few changes to the MATLAB program for each case, therefore it is more useful and adaptable for the engineering design, especially for LED engineers since they are not familiar with the heat transfer.

4. Spreading resistance analysis

According to equation (10), the temperature change has a strong relation with heat source locations. A program was built to calculate the total temperature distribution in the LED heat sink plate. In this program, five hundreds and seventy points on heat sink base are picked out to calculate their temperatures. These points uniformly locate on heat sink base in an array with thirty columns and nineteen rows. The program can easily find the highest and the lowest temperature points. The result shows temperature difference of the hottest point and the coldest point on heat sink base changes greatly when heat sources locations change. Table 2 clearly demonstrates this viewpoint. In Table 2, it is found that for different LEDs distribution, maximal temperature differences among the heat sink base change from 5.5 °C to 12.1 °C. It is obvious that LED chip distribution greatly affects the spreading thermal resistance of the present multi-chip LED street lamp. Figs. 6 and 7 show the temperature field of one chip distribution case, where the maximal temperature difference is 5.5 °C. It is found that chip distribution or the heat sources distribution has an obvious influence on temperature uniformity or the spreading thermal resistance of the heat sink base. This proves that the spreading thermal resistance cannot be neglected in multiple chip packaging like the present 80 W LED street lamp.

Table 4
Coordinates of all chip locations.

X coordinate of the chip locations					
Old	0.14	0.22	0.3	0.38	0.46
New	0.06	0.18	0.3	0.42	0.54
Y coordinate of the chip locations					
Old	0.015	0.055	0.095	0.135	
New	0.022	0.056	0.124	0.188	

5. Temperature field optimization

From the isothermal charts shown in Figs. 6 and 7, it is obvious that there is a temperature difference on the plate. It is nearly 5 °C temperature difference. Besides the LED chip locations, temperatures of the middle and lowest parts of the plate are also high. Therefore, the temperature uniformity of the heat sink for the LED street lamp is not satisfactory. It is known that the temperature gradient is very harmful to LED reliability because of the thermal stress. For multi-chip packaging structures, according to the above discussions, changing the location of LED chips is a good method to obtain better temperature uniformity. In order to realize the optimization process, the maximal temperature difference existing on the heat sink plate is defined as objective function.

To find out the optimized chip distance at X coordinate, a loop is used in the calculation program in which the X coordinates of the chips changes incrementally each time. In this case, the chip locations are changed, which are shown in Table 3. In the result shown in Fig. 8, the highest temperature becomes lower. Temperature of the location under 5 W chips is 45.1 °C, and temperature of the location under 3 W chips is 43.5 °C. The temperature difference between 5 W chips and 3 W chips are 1.6 °C. The highest temperature in the model has decreased sharply. The lowest temperature of the plate increases, which has raised nearly 6 °C. Temperature uniformity has an obvious improvement compared with the case shown in Figs. 3 and 4.

In Fig. 8, it is noted that there are still temperature differences between different rows. Therefore, the chip arrangement needs to be treated with further optimization. Here, to realize the above target, compared with the last case, the new calculation program adds another loop to change both the X and Y coordinates together. Finally, the new chip distribution is shown in Table 4, the corresponding temperature field is shown in Fig. 9. It is found from Fig. 9 that temperatures of the 5 W chip locations are 44.8 °C, and temperatures of 3 W chip locations are 43.5 °C. The temperature difference on the board is just 2.21 °C. Comparing with the temperature difference in the last optimization, the chip arrangement is much better.

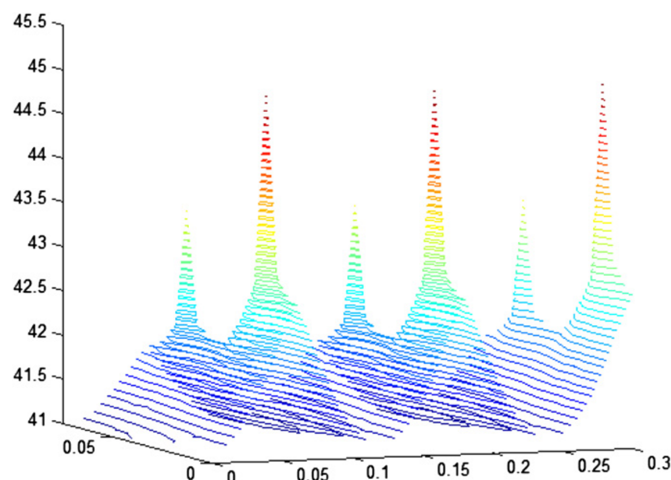

Fig. 8. Temperature field of one optimization case.

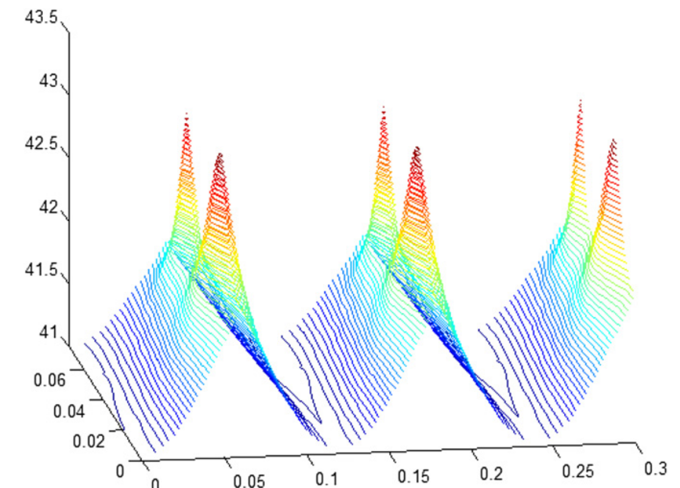

Fig. 9. Temperature field of an optimized chip distribution case.

6. Conclusions

A general analytical solution is introduced to analyze the spreading thermal resistance and temperature distribution of multi-chip LED packaging in this study. The previous results obtained by the experiment of the 80 W LED street lamp, and its numerical analysis are used to compare with those by this general analytical method. The comparison proves that the analytical solution is effective. Based on the temperature distribution analysis, it is found that the spreading resistance strongly depends on the LED chip distribution. Spreading thermal resistance has an important role in thermal optimization of a multiple LED packaging. In order to achieve uniform temperature distribution, the optimization based on the general analytical solution has been conducted with the maximal temperature difference as an objective function, the results shows that it can conveniently provide the optimized chips distribution.

Acknowledgments

This work was supported by National Natural Science Foundation of China (No. 50876038, 50835005).

References

[1] M. Alan, Solid state lighting-a world of expanding opportunities at LED 2002, III–V Review 16 (1) (2003) 30–33.
[2] X.B. Luo, T. Cheng, W. Xiong, Z.Y. Gan, S. Liu, Thermal analysis of an 80 W light-emitting diode street lamp, IET Optoelectronics 1 (5) (2007) 191–196.
[3] S.L. Chuang, A. Ishibashi, S. Kijima, N. Nakayama, M. Ukita, S. Taniguchi, Kinetic model for degradation of light-emitting diodes, IEEE Journal of Quantum Electronics 33 (6) (1997) 970–979.
[4] L. Kim, M.W. Shin, Thermal analysis and design of high power LED packages and systems, Proceedings of SPIE 6337 (2006) 63370U-1–63370U-9.
[5] S. Lee, S. Song, V. Au, K.P. Moran, Constriction/spreading resistance model for electronics packaging, in: Proceedings of ASME/JSME Thermal Engineering Conference, vol. 4, 1995, pp. 199–206.
[6] M. Grujicic, C.L. Zhao, E.C. Dusel, The effect of thermal contact resistance on heat management in the electronic packaging, Applied Surface Science 246 (2005) 290–302.
[7] T.M. Ying, K.C. Toh, A constriction resistance model in thermal analysis of solder ball joints in ball grid array packages HTD, Proceedings of the ASME 364-1 (1995) 29–36.
[8] Y.S. Muzychka, J.R. Culham, M.M. Yovanovich, Thermal spreading resistance of eccentric heat sources on rectangular flux channels, ASME Journal of Electronic Packaging 125 (2003) 178–185.
[9] M.M. Yovanovich, Y.S. Muzychka, J.R. Culham, Spreading resistance of isoflux rectangles and strips on compound flux channels, AIAA Journal of Thermophysics and Heat Transfer 13 (4) (1999) 495–500.
[10] M.M. Yovanovich, J.R. Culham, P. Teertstra, Analytical modeling of spreading resistance in flux tubes, half spaces and compound disks, IEEE Transactions on Components, Packaging, and Manufacturing Technology-Part A 21 (1) (1998) 168–176.
[11] M.M. Yovanovich, C.H. Tien, G.E. Schneider, General Solution of Constriction Resistance within a Compound Disk, Progress in Astronaut-Tics and Aeronautics: Heat Transfer, Thermal Control, and Heat Pipes, MIT Press, Cambridge, MA, USA, 1980, pp. 47–62.
[12] Y.S. Muzychka, C.M. Stevanovi, M.M. Yovanovich, Thermal spreading resistances in compound annular sectors, AIAA Journal of Thermophysics and Heat Transfer 15 (3) (2001) 354–359.
[13] T.T. Lam, W.D. Fischer, Thermal resistance in rectangular orthotropic heat spreaders, ASME Advances in Electronic Packaging 26-1 (1999) 891–898.
[14] T.M. Ying, K.C. Toh, A heat spreading resistance model for anisotropic thermal conductivity materials in electronic packaging, Proceedings of the Seventh Intersociety Conference on Thermal and Thermomechanical Phenomena in Electronic Systems 1 (2000) 314–321.
[15] Y.S. Muzychka, M.M. Yovanovich, J.R. Culham, Thermal spreading resistance in rectangular flux channels, part I: geometric equivalences, AIAA Paper 2003–4187, 2003.
[16] Y.S. Muzychka, J.R. Culham, M.M. Yovanovich, Thermal spreading resistance in rectangular flux channels: part II edge cooling, AIAA Paper 2003-4188, 2003.
[17] M.M. Yovanovich, Thermal resistances of circular source on finite circular cylinder with side and end cooling, ASME Journal of Electronic Packaging 125 (2003) 169–177.
[18] Y.S. Muzychka, Influence coefficient method for calculating discrete heat source temperature on finite convectively cooled substrates, IEEE Transactions on Components and Packaging Technologies 29 (3) (2006) 636–643.
[19] A. Christensen, S. Graham, Thermal effects in packaging high power light emitting diode arrays, Applied Thermal Engineering 29 (2009) 364–371.
[20] S. Chhajed, Y. Xi, Th. Gessmann, J.Q. Xi, J.M. Shah, J.K. Kim, E.F. Schubert, Junction temperature in light-emitting diodes assessed by different methods, Proceedings of SPIE 5739 (2005) 16–24.
[21] S. Todorki, M. Sawai, K. Aiki, Temperature distribution along the striped active region in high-power GaAlAs visible lasers, Journal of Applied Physics 58 (3) (1985) 1124–1128.
[22]. P.W. Epperlein, G.L. Bona, Influence of the vertical structure on the mirror facet temperatures of visible GaInP quantum well laser, Applied Physics Letter 62 (1993) 3074–3076.